P H Y S I C A L   R E V I E W   L E T T E R S

Correlation between the Superconducting Transition Temperature and Anisotropic Quasiparticle Scattering in $Tl_2Ba_2CuO_{6+\delta}$

M. Abdel-Jawad,[1] J. G. Analytis,[1] L. Balicas,[2] A. Carrington,[1] J. P. H. Charmant,[3] M. M. J. French,[1] and N. E. Hussey[1]

[1]*H. H. Wills Physics Laboratory, University of Bristol, Bristol BS8 1TL, United Kingdom*
[2]*National High Magnetic Field Laboratory, Florida State University, Tallahassee, Florida 32306, USA*
[3]*The School of Chemistry, University of Bristol, Bristol BS8 1TS, United Kingdom*

Angle-dependent magnetoresistance measurements are used to determine the isotropic and anisotropic components of the transport scattering rate in overdoped $Tl_2Ba_2CuO_{6+\delta}$ for a range of T_c values between 15 and 35 K. The size of the anisotropic scattering term is found to scale linearly with T_c, establishing a link between the superconducting and normal state physics. A comparison with results from angle resolved photoemission spectroscopy indicates that the transport and quasiparticle lifetimes are distinct.

Understanding the normal state is regarded as a key step in resolving the problem of high temperature superconductivity (HTSC), yet establishing any clear correlation between the two has proved difficult. Most empirical correlations to date, such as the Uemura plot [1] and the linear scaling of the magnetic resonance mode energy with T_c [2], are associated with the superconductivity. Homes' law, linking T_c with the product of the superfluid density and the dc conductivity (at T_c) [3], is a rare example of a correlation linking the two states, though this also could be viewed as a consequence of superconducting (SC) gap formation rather than a normal state property [4]. Transport properties, particularly for current in-plane, appear very much tied to the T_c parabola (for a review see [4]) but any direct correlation between transport and superconductivity has not yet been found. Finally, the precise doping dependence of the pseudogap and its relation to T_c remains a controversy [5].

Here we identify a new correlation between the normal and superconducting states using a bulk transport probe, namely, interlayer angle-dependent magnetoresistance (ADMR) [6]. ADMR has provided detailed Fermi surface (FS) information for a variety of one- and two-dimensional (2D) metals [7–9]. Recently the technique was extended to incorporate basal-plane anisotropy and to reveal the temperature T and momentum (**k**) dependence of the scattering rate $\Gamma(T, \mathbf{k})$ in heavily overdoped (OD) $Tl_2Ba_2CuO_{6+\delta}$ (Tl2201) [10]. There $\Gamma(T, \mathbf{k})$ was found to consist of two components, one isotropic and quadratic in T, the other anisotropic, maximal near the saddle points at $(\pi, 0)$ and proportional to T.

In this Letter, ADMR measurements at $T = 40$ K and magnetic field $\mu_0 H = 45$ T are compared for a number of OD Tl2201 crystals with T_c values between 15 and 35 K. The strength of the anisotropic scattering extracted from the analysis is found to scale linearly with T_c, appearing to extrapolate to zero at the doping level where superconductivity vanishes. This finding implies that the anisotropic scattering mechanism is intimately related to the mechanism of HTSC. In marked contrast to recent results from angle resolved photoemission spectroscopy (ARPES) [11,12], no sign reversal of the anisotropy in the quasiparticle lifetime is inferred. Finally, our results shed new light on the doping evolution of both the in-plane resistivity $\rho_{ab}(T)$ and the Hall coefficient $R_H(T)$ in OD cuprates.

For this study a total of six self-flux grown crystals (typical dimensions $0.3 \times 0.3 \times 0.03$ mm³) were annealed at temperatures $300\,°C \leq T \leq 600\,°C$ in flowing O_2 and mounted in a c-axis quasi-Montgomery configuration. The ADMR were measured on a two-axis rotator in the 45 T hybrid magnet at the National High Magnetic Field Laboratory in Florida using a conventional four-probe ac lock-in technique. The orientation of the crystal faces was indexed for a number of crystals using a single crystal x-ray diffractometer.

The first and third panels of Fig. 1 show polar ADMR data $\Delta\rho_\perp/\rho_\perp(0)$ (normalized to their zero-field value) at different azimuthal angles ϕ (relative to the Cu-O-Cu bond direction) for two crystals Tl15Kb and Tl32K (the numbers relate to their T_c values). Though the two sets of data look similar, there are some key differences [13]. First $\Delta\rho_\perp/\rho_\perp(0)$ is significantly larger for the lower T_c crystal. Second, for polar angles $|\theta| \sim \pi/2$, Tl32K shows much less ϕ-dependence and finally, near $\mathbf{H} \parallel c$ ($\theta = 0$), the Tl15Kb curves are more rounded. As shown below, these features are caused by the higher T_c, less overdoped sample(s) possessing a significantly larger basal-plane anisotropy in $\omega_c\tau$ (the product of the cyclotron frequency and the transport lifetime).

In order to extract information on the FS and $\omega_c\tau$, we carried out a least-square fitting of the data using the Shockley-Chambers tube integral form of the Boltzmann transport equation modified for a quasi-2D metal with a fourfold anisotropic scattering rate $1/\tau(\varphi) = (1 + \alpha\cos4\varphi)/\tau^0$ and anisotropic in-plane velocity $v_F(\varphi)$, incorporated via $1/\omega_c(\varphi) = (1 + \beta\cos4\varphi)/\omega_c^0$ [10,14]. The sign of α defines the location of maximal scattering. The FS wave vector $k_F(\theta, \varphi)$ was parameterized by the
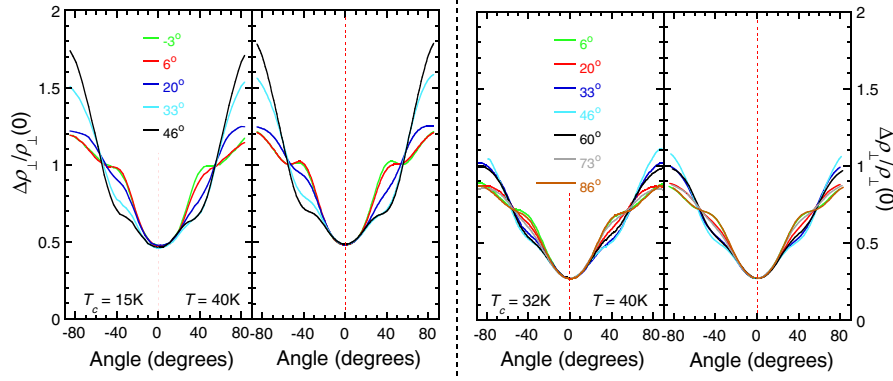
FIG. 1 (color online). Angle-dependent magnetoresistance sweeps for two overdoped Tl2201 single crystals with T_c of 15 K (Tl15Kb—left side) and 32 K (Tl32K—right side) measured at 40 K and 45 T. The least-square fits to the data are displayed on the right of each plot. The labels refer to the azimuthal angle of the magnetic field with respect to the Cu-O-Cu bond direction.

lowest-order harmonic components satisfying the body-centered-tetragonal symmetry of Tl2201 [8],

$$k_F(\theta, \varphi) = k_{00} - k_{40}\cos4\varphi - k_{21}\cos(k_z c/2)\sin2\varphi$$
$$- k_{61}\cos(k_z c/2)\sin6\varphi - k_{101}\cos(k_z c/2)$$
$$\times \sin10\varphi, \qquad (1)$$

where k_z is the c-axis wave vector and c the interlayer spacing. An eightfold term $k_{80}\cos(8\varphi)$ had a negligible effect on the parameterization and was therefore not included in the fitting procedure. Note that the c-axis warping parameters k_{21}, k_{61}, and k_{101} are small compared to k_{00}, the radius of the cylindrical FS (about the zone corners), and k_{40}, its in-plane squareness, and only ratios (e.g., k_{61}/k_{21}) can be determined to good accuracy. To minimize the number of free parameters, we fix $k_{101}/k_{21} = k_{61}/k_{21} - 1$ such that $t_\perp(\varphi)$ vanishes at $\varphi = 0°$ and $45°$ [9,15] and fix k_{00} using the empirical relation $T_c/T_c^{\max} = 1 - 82.6(p - 0.16)^2$ with $T_c^{\max} = 92$ K and $(\pi k_{00}^2)/(2\pi/a)^2 = (1 + p)/2$ [16]. β depends largely on our choice of k_{61}/k_{21} with the best least-square values giving $\beta = 0 \pm 0.1$ for $0.6 \le k_{61}/k_{21} \le 0.8$ for all samples [17]. The sum $\alpha + \beta$ was much less sensitive to variations in k_{61}/k_{21} and for simplicity, we assume hereafter $\omega_c(\varphi) = \omega_c^0$. For completeness however, in Table I we list the values for $\alpha + \beta$.

TABLE I. Parameters obtained from the least-square fitting of AMRO data for six different Tl2201 crystals at 40 K. Errors given in parentheses determine the error bars in Fig. 2.

T_c	$k_{00}(\text{Å}^{-1})$	$k_{40}(\text{Å}^{-1})$	k_{61}/k_{21}	$\omega_c^0\tau^0$	$\alpha + \beta$
15 K	0.730	0.038(3)	0.73(8)	0.27(1)	0.31(2)
15 K	0.730	0.034(3)	0.71(13)	0.28(2)	0.32(3)
17 K	0.729	0.035(3)	0.68(12)	0.29(2)	0.29(3)
20 K	0.728	0.033(3)	0.67(10)	0.26(2)	0.36(4)
32 K	0.726	0.037(3)	0.67(10)	0.21(2)	0.42(3)
35 K	0.725	0.030(3)	0.71(11)	0.21(2)	0.45(3)

The best fits, shown in the panels to the right of each data set, are all excellent and the four remaining fitting parameters displayed in Table I appear well constrained due to the wide range of polar and azimuthal angles studied [18]. Within our experimental resolution, the FS parameters appear to have negligible doping dependence. Moreover, the projected in-plane FS is found to be in good agreement with a recent ARPES study on the same compound [12]. The anisotropy parameter α increases with rising T_c while $\omega_c^0\tau^0$ shows the opposite trend (reflecting the overall reduction in the ADMR in Fig. 1).

Our previous analysis of Tl15Ka implied the existence of both isotropic and anisotropic components in the scattering rate in OD Tl2201 [10]. Accordingly we split $1/\omega_c^0\tau(\varphi)$ into two components $\gamma_{\text{iso}} = (1 - \alpha)/\omega_c^0\tau^0$ and $\gamma_{\text{aniso}} = 2\alpha/\omega_c^0\tau^0\cos^2 2\varphi$. In Tl15Ka, $\gamma_{\text{iso}} \sim A + BT^2$, due to a combination of impurity and electron-electron scattering, while $\gamma_{\text{aniso}} \sim CT$ (setting $\beta = 0$) [10], the microscopic origin of which has yet to be identified. The doping (T_c) dependence of γ_{iso} and γ_{aniso} (at $T = 40$ K) are shown in the top and bottom panels of Fig. 2, respectively. Although we cannot say anything about the T dependence of the two components, it is clear that while γ_{iso} is essentially doping independent, γ_{aniso} shows a clear linear scaling with T_c, extrapolating to zero at the onset of superconductivity (on the OD side). Within a standard rigid band model, one would expect anisotropy in $v_F(\varphi)$ and hence in $\omega_c(\varphi)$ to increase with doping as the FS at the Brillouin zone boundary approaches the saddle points. The fact that the data show the opposite trend is therefore significant and justifies our key assumption that the basal-plane anisotropy in Tl2201 is dominated by anisotropy in $1/\tau(\varphi)$ [10,17], which, surprisingly for such highly OD samples, remains significant (the absolute anisotropy $\gtrsim 2$ for Tl35K at $T = 40$ K).

This empirical correlation between γ_{aniso} and T_c has several implications for the normal state of OD cuprates. First, given that the carrier concentration is varying only weakly (as $1 + p$) in this doping range, it is apparent that
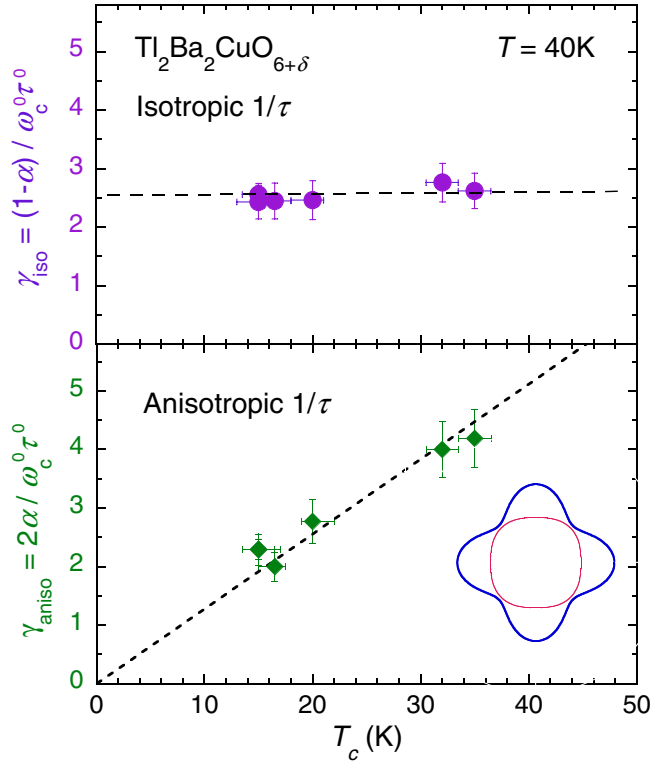
FIG. 2 (color online). Top. Doping dependence of $\gamma_{\mathrm{iso}} \equiv (1 - \alpha)/\omega_c^0 \tau^0$ at $T = 40$ K. Bottom. Doping dependence of $\gamma_{\mathrm{aniso}} \equiv 2\alpha/\omega_c^0 \tau^0$ at $T = 40$ K and $\varphi = 0$. Here we have assumed $\beta = 0$. For $\beta = \pm 0.1$ (our range of uncertainty in β), the γ_{iso} (γ_{aniso}) points are shifted by ± 0.4 (∓ 0.4), respectively. Inset: In-plane variation of γ_{aniso} (thick blue line) with respect to $k_F(\varphi)$ (thin red line).

the marked change in the absolute value of resistivity with doping [19] is due primarily to a decrease in anisotropic scattering. Second, the observation of cyclotron motion over the full FS volume implies that there are no pseudo-gapped regions of FS in OD Tl2201 for $x \gtrsim 0.24$ [5]. Whilst one might argue that such a large applied field could suppress any pseudogapping in our crystals [20], our conclusion is consistent with the observation of metal-lic $\rho_\perp(T)$ in zero field [9,21]. The c-axis pseudogap, inferred from interlayer tunnelling [20] and scanning tun-neling microscopy [22] on $Bi_2Sr_2CaCu_2O_{8+\delta}$, is therefore a nonuniversal feature of OD cuprates.

Last, and most important, the suppression of supercon-ductivity on the OD side looks to coincide with the dis-appearance of γ_{aniso}. This conclusion is consistent with the observation in nonsuperconducting $La_{1.7}Sr_{0.3}CuO_4$ of a strictly T^2 resistivity [23] (provided γ_{aniso} remains T lin-ear) and a vanishing of T dependence of the resistive anisotropy $\rho_\perp/\rho_{ab}(T)$ [24,25] and indicates an intimate relation between the anisotropic scattering and HTSC. Our findings contrast markedly with the doping evolution of the imaginary part of the quasiparticle self-energy ImΣ in-ferred from ARPES. Here the nodal/antinodal quasiparticle anisotropy is seen to vanish [26] or even reverse its sign

[11,12] before superconductivity is suppressed on the OD side. ARPES-specific issues such as resolution, back-ground subtraction and matrix-element effects are not believed to be important here [27]. One thus needs to ask the question whether the two probes are in fact measuring the same quantity. Direct comparison of the scattering rates deduced from ADMR (this study and Ref. [21]) and ARPES [12] in Tl2201 ($T_c \sim 30$ K) shows that the former is more than 1 order of magnitude smaller. Since ARPES measures the quasiparticle lifetime, small-angle scattering must contribute significantly to ImΣ. Interlayer transport in cuprates, however, is also believed to be determined by a product of single-particle spectral functions on adjacent planes [28] and may thus be similarly susceptible to small-angle scattering. Given that ADMR is a bulk probe, we conjecture that the anomalously large linewidths seen in ARPES most probably arise from additional scattering at the (cleaved) surface.

As stated above, $\gamma_{\mathrm{aniso}}(T)$ could account for both $R_H(T)$ and $\rho_{ab}(T)$ in Tl15Ka at low T [10]. To simulate the doping evolution of $\rho_{ab}(T, p)$ and $R_H(T, p)$ in Tl2201, we adopt a simple one-parameter-scaling model and calculate ρ_{ab}, R_H (and the in-plane magnetoresistance $\Delta\rho_{ab}/\rho_{ab}$) using the Jones-Zener form of the Boltzmann equation for a quasi-2D FS [29]. First, k_{40} and k_{00} are fixed using the values for Tl15Ka listed in Table I and the scaling relation [16] described earlier. Second, we assume that $1/\omega_c\tau(T, \varphi)$ has the same form as Tl15Ka for all crystals, i.e., $1/\omega_c\tau(T, \varphi) = \gamma_{\mathrm{iso}}(T) + \gamma_{\mathrm{aniso}}(T, \varphi) = A + BT^2 + C(p)T\cos^2 2\varphi$, where $C(p) = C(\mathrm{Tl15Ka})T_c(p)/15$ [10]. Finally, the anticipated return to isotropic scattering at high T is simulated by inclusion (in parallel) of a maximum scattering rate $\Gamma_{\mathrm{max}} = \langle v_F(\varphi) \rangle / a$ (where a is the in-plane lattice spacing) in accord with the Ioffe-Regel limit [29]. In this way, $\gamma(T, \varphi)$ saturates at different points on the FS at different T. Such anisotropy in the onset of saturation (of Im$\Sigma(\omega)$) has been seen in optimally doped $La_{2-x}Sr_xCuO_4$ [30].

The resultant simulations for $R_H(T, p)$ and $\rho_{ab}(T, p)$ are presented in Fig. 3 for $T_c = 10, 25, 50,$ and 80 K. Despite there being no free parameters ($C(p)$ is fixed by T_c), the $R_H(T)$ plots show qualitative agreement with the published data (solid symbols, [19,21,31]). The p dependence of $\rho_{ab}(T)$ is also consistent with experiment, where the ex-ponent n of ρ_{ab} ($= \rho_0 + \nu T^n$) is found to evolve smoothly from 1 to 2 between optimal doping and the SC/non-SC boundary [19]. Finally, $\Delta\rho_{ab}/\rho_{ab}$ (top left panel for $T_c = 25$ K) displays the correct magnitude and T dependence [21]. This correspondence, plus the fact that our simulations capture the marked increase in the magni-tude of R_H for what are relatively small changes in carrier concentration, suggests that anisotropic scattering is a dominant contributor to the T and p dependence of R_H across the OD regime, while the monotonic variation of $R_H(T, p)$ is incompatible with a sign reversal of the scat-tering rate anisotropy near $p = 0.2$ inferred from ARPES [11,12].
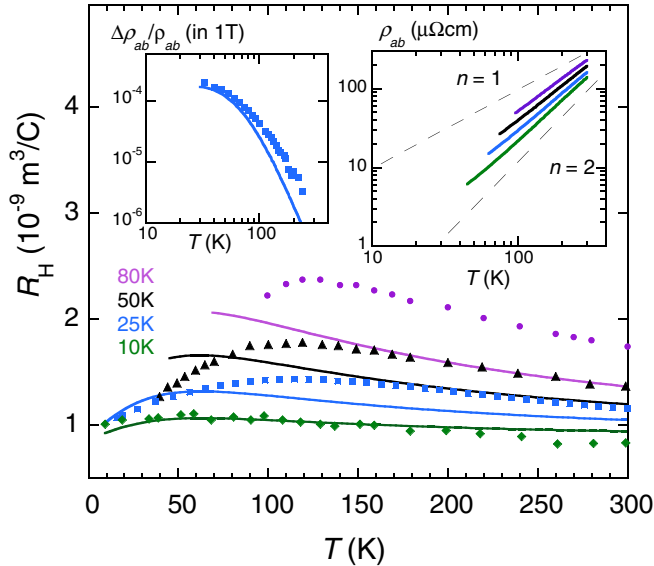
FIG. 3 (color online). Main: $R_H(T)$ simulations for Tl2201 with T_c values of 10, 25, 50, and 80 K (solid lines) together with published data for 10 K (green diamonds [31]), 25 K (blue squares [21]), and 50 K (black triangles [31]) single crystals plus polycrystalline data for $T_c = 81$ K (purple circles, [19]). Top right. Simulation of $\rho_{ab}(T) - \rho_{ab}(T = 0)$ (on a log-log scale) using the same parameterization. Top left—Solid line: Simulation of $\Delta\rho_{ab}/\rho_{ab}(T)$ at 1 T for $T_c = 25$ K. Blue squares: $\Delta\rho_{ab}/\rho_{ab}(T)$ data at 1 T for $T_c = 25$ K crystal [21].

As for possible origins of the observed anisotropy, real-space (correlated) electronic inhomogeneity [32] is one possible candidate though as yet, no measurements have been performed on heavily OD non-SC cuprates to establish any possible link between inhomogeneity and superconductivity. Interactions with a bosonic mode are another possibility, though given the strong angle and doping dependence, presumably not phonons. More likely candidates include spin, charge (stripe), or d-wave pairing fluctuations which all disappear with superconductivity on the OD side [25,33,34]. The preservation of the T-linear scattering rate to low T though implies a vanishingly small energy scale for such fluctuations, characteristic of proximity to a quantum critical point. Intriguingly, the transport scattering rate close to a 2D Pomeranchuk instability was recently shown to have a form identical to that observed in OD Tl2201 [35]. In such a scenario however, γ_{aniso} should strengthen, rather than diminish, with doping as the van Hove singularity is approached on the OD side.

In conclusion, we have found a correlation between T_c and the anisotropy of the transport scattering rate in OD Tl2201. Although necessarily focused on heavily OD cuprates, this observation has implications for the entire phase diagram, in particular, the evolution of $R_H(T, p)$. In addition, the present results support a previously unforeseen link between the normal state scattering and superconducting mechanisms. Finally, our ADMR results affirm that

maximal scattering remains at the antinodes throughout the OD region, in contrast to what has been recently inferred from ARPES measurements.

[1] Y. J. Uemura *et al.*, Phys. Rev. Lett. **62**, 2317 (1989).
[2] H. He *et al.* Phys. Rev. Lett. **86**, 1610 (2001).
[3] C. C. Homes *et al.*, Nature (London) **430**, 539 (2004).
[4] N. E. Hussey, in *Handbook of High Temperature Superconductivity: Theory and Experiment*, edited by J. R. Schrieffer (Springer-Verlag, Amsterdam, 2007).
[5] J. L. Tallon and J. W. Loram, Physica (Amsterdam) **C349**, 53 (2001).
[6] K. Yamaji, J. Phys. Soc. Jpn. **58**, 1520 (1989).
[7] M. V. Kartsovnik, Chem. Rev. **104**, 5737 (2004).
[8] C. Bergemann *et al.*, Adv. Phys. **52**, 639 (2003).
[9] N. E. Hussey *et al.*, Nature (London) **425**, 814 (2003).
[10] M. Abdel-Jawad *et al.*, Nature Phys. **2**, 821 (2006).
[11] X. J. Zhou *et al.* Phys. Rev. Lett. **92**, 187001 (2004).
[12] M. Platé *et al.*, Phys. Rev. Lett. **95**, 077001 (2005).
[13] The asymmetry around $\theta = 0$ arises from slight misalignment of the crystalline c axis with respect to the rotational platform. The inclusion of a coordinate axis rotated around the platform axis can account for such a distortion and has been added to our fitting routine though has a negligible effect on the parameters obtained.
[14] Similar results are obtained for weakly incoherent layers, M. P. Kennett and R. H. McKenzie, Phys. Rev. B **76**, 054515 (2007).
[15] O. K. Andersen *et al.*, J. Phys. Chem. Solids **56**, 1573 (1995).
[16] M. R. Presland *et al.*, Physica (Amsterdam) **C176**, 95 (1991).
[17] J. G. Analytis *et al.*, arXiv:0708.1666v1.
[18] Note for Tl15Ka, top line in Table I, data have been obtained for only one azimuthal angle [10].
[19] Y. Kubo *et al.*, Phys. Rev. B **43**, 7875 (1991).
[20] T. Shibauchi *et al.*, Phys. Rev. Lett. **86**, 5763 (2001).
[21] N. E. Hussey *et al.*, Phys. Rev. Lett. **76**, 122 (1996).
[22] C. Renner *et al.*. Phys. Rev. Lett. **80**, 149 (1998).
[23] S. Nakamae *et al.*, Phys. Rev. B **68**, 100502(R) (2003).
[24] Y. Nakamura and S. Uchida, Phys. Rev. B **47**, 8369 (1993).
[25] L. B. Ioffe and A. J. Millis, Phys. Rev. B **58**, 11 631 (1998).
[26] K. Yang *et al.*, Phys. Rev. B **73**, 144507 (2006).
[27] D. C. Peets *et al.*, New J. Phys. **9**, 28 (2007).
[28] K. G. Sandemann and A. J. Schofield, Phys. Rev. B **63**, 094510 (2001).
[29] N. E. Hussey, Eur. Phys. J. B **31**, 495 (2003).
[30] J. Chang *et al.*, Phys. Rev. B **75**, 224508 (2007).
[31] T. Manako, Y. Kubo, and Y. Shimakawa, Phys. Rev. B **46**, 11 019 (1992).
[32] K. McElroy *et al.*, Phys. Rev. Lett. **94**, 197005 (2005).
[33] S. Wakimoto *et al.*, Phys. Rev. Lett. **92**, 217004 (2004).
[34] D. Reznik *et al.*, Nature (London) **440**, 1170 (2006).
[35] L. Dell'Anna and W. Metzner, Phys. Rev. Lett. **98**, 136402 (2007).